Tuning martensitic transformation and magnetoresistance effect by low temperature annealing in $Ni_{45}Co_5Mn_{36.6}In_{13.4}$ alloys

2011 J. Phys. D: Appl. Phys. 44 085002

(http://iopscience.iop.org/0022-3727/44/8/085002)

J. Phys. D: Appl. Phys. **44** (2011) 085002 (5pp) doi:10.1088/0022-3727/44/8/085002

Tuning martensitic transformation and magnetoresistance effect by low temperature annealing in $Ni_{45}Co_5Mn_{36.6}In_{13.4}$ alloys

L Chen[1], F X Hu[1], J Wang[1], J L Zhao[1], J R Sun[1], B G Shen[1], J H Yin[2] and L Q Pan[2]

[1] State Key Laboratory for Magnetism and Beijing National Laboratory for Condensed Matter Physics, Institute of Physics, Chinese Academy of Sciences, Beijing 100190, People's Republic of China
[2] Department of Physics, University of Science and Technology Beijing, Beijing 100083, People's Republic of China

E-mail: hufx@g203.iphy.ac.cn

Received 23 September 2010, in final form 21 December 2010
Published 10 February 2011
Online at stacks.iop.org/JPhysD/44/085002

Abstract
We studied the influence of post-annealing on magnetic and transport properties in $Ni_{45}Co_5Mn_{36.6}In_{13.4}$ alloys. Our results demonstrate that post-annealing at low temperatures, $\leqslant$300 °C, can lead to a significant change in magnetic properties, martensitic temperature (T_M) and magnetoresistance effect through structure relaxations and possible change in atomic order. It was found that T_M shifts from 314 to 283 K but the strong metamagnetic behaviour is still retained when the sample is annealed at 300 °C for 3 h. Thereupon, a large magnetoresistance effect over an extended temperature range can be achieved through controlling the heat treatment conditions. Meanwhile, the thermal stability of the novel composition is also disclosed through the investigations on low temperature annealing effect.

1. Introduction

Increasing attention has been given to the magnetoresistance (MR) effect because of extensive applications in magneto-resistive reading heads and related devices. Giant magneto-resistance (GMR) and colossal magnetoresistance (CMR) effects have been discovered in magnetic multilayers and perovskite manganites [1, 2]. Additionally, considerable MR effect was also observed in many intermetallic compounds [3, 4], particularly for the ones undergoing first-order transitions. Apart from understanding the basic mechanism of the MR effect in different systems, much effort has been concentrated on obtaining a large room-temperature MR considering the practical applications.

The metamagnetic Heusler alloys with exact composition $Ni_{45}Co_5Mn_{36.6}In_{13.4}$ are well known for the huge shape memory effect [5, 6]. The underlying mechanism is different from the conventional ferromagnetic Heusler alloys, in which the ferromagnetic shape memory effect results from the field-induced rearrangement of martensite variants. In metamagnetic Heusler alloys, however, an abrupt change in magnetization across the martensitic transition results in a large Zeeman energy $\mu_0 \Delta M \cdot H$, which drives a metamagnetic transition behaviour. The co-occurred structural transformation is accompanied with a huge shape memory effect. The incorporation of Co in these alloys enhances the Zeeman energy $\mu_0 \Delta M \cdot H$ through enlarging the magnetization difference across the martensitic transformation, thus an extremely large stress is generated by magnetic field. The stress output in $Ni_{45}Co_5Mn_{36.6}In_{13.4}$ can be over 100 MPa under a 7 T field [5], which is approximately 50 times larger than that in conventional Heusler alloys. Along with field-induced metamagnetic behaviours, large magnetocaloric effect (MCE) [7] and magnetoresistance (MR) [8, 9] were also observed in this kind of novel materials. In order to exploit these functions in a wide temperature range, people tune T_M arbitrarily while keeping strong metamagentic properties, in the meantime obtaining large MCE, MR and huge shape memory effect.

Normally the method to tune T_M is to adjust valence electron concentration (e/a) through changing the compositions or introducing other elements. However, such a method could bring additional negative effect in some cases. It has been reported that T_M not only depends on e/a but also relates to the species of the dopant atom [10], i.e. atomic mass and radius [11], due to the strong effect of electron–phonon coupling. Thus, the introduction of dopant atoms sometimes makes the issue complicated when the effect of the alteration of e/a contradicts that of the mean atomic mass and radius variation after the introduction of dopant atoms.

Here, we report a different route to tune T_M and the magnetoresistance effect in $Ni_{45}Co_5Mn_{36.6}In_{13.4}$ alloys. Recent investigations [12, 13] indicated that additional annealing at relatively high temperatures, $\geqslant$350 °C, for the as-prepared Ni–Co–Mn–In metamagnetic alloys, can lead to changes in structure, martensitic transformation and metamagnetic behaviours through influencing atomic ordering. It was noted that T_M and metamagnetic behaviour sometimes disappear upon annealing due to the kinetic arrest effect [12]. Recently, we carried out the investigations of low-temperature annealing effect on magnetic properties, martensitic transformation and the magnetoresistance effect. Our studies indicate that proper annealing at low temperatures, $\leqslant$300 °C, can tune T_M around room temperature while keeping the strong metamagnetic properties unchanged, thus a large MR effect can be realized over an extended temperature range around room temperature. The as-prepared samples contain stress since they quenched from 1173 K to ice water at the end of preparation. Subsequently annealing even at a low temperature can relax the stress and modify atomic ordering, Mn–Mn distance, as well as lattice symmetry. As a result, the Mn–Mn exchange coupling, Brillouin zone boundary and thus the T_M can be changed. Our studies on the low-temperature annealing effect also reveal thermal stabilities of the novel compositions.

2. Experimental procedure

$Ni_{45}Co_5Mn_{36.6}In_{13.4}$ alloys were prepared by the arc-melting technique. The commercial purities of Ni, Mn, Co, In are 99.999 wt%, 99.9 wt%, 99.9 wt% and 99.995 wt%, respectively. The obtained ingots were each wrapped with Ta foil and homogenized in a sealed quartz tube at 1173 K for 24 h, then quenched in ice water. The preparation process is in accord with the report in [5]. The obtained samples are denoted as sample O. Subsequently, the samples were further vacuum annealed for 3 h at 250 °C and 300 °C and then quenched in ice water. The resulting samples are denoted as sample 250 and sample 300, respectively. Our experiments demonstrate that the as-prepared sample is stable. Annealing at temperatures lower than 200 °C cannot cause any changes in structure, transition temperatures and magnetic properties. However, the samples begin to lose stability once the annealing temperature reaches 250 °C, and significant changes in magnetic and transport properties take place. Magnetic and transport measurements were performed using a superconducting quantum interference device (SQUID) equipped with a probe for four-point electrical resistance (R) measurements.

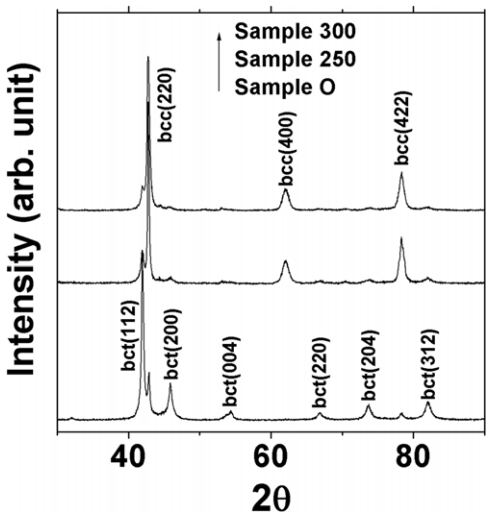

Figure 1. X-ray diffraction patterns collected at room temperature for sample O (fresh sample), sample 250 (annealed at 250 °C for 3 h) and sample 300 (annealed at 300 °C for 3 h).

3. Results and discussion

Figure 1 shows the results of x-ray diffraction (XRD) measurements by using Cu Kα radiation. At room temperature the sample O exhibits a body-centred tetragonal (bct) martensitic structure with admixture of a small amount of body-centred cubic (bcc) austenitic structure, while the other two show bcc austenitic structure with admixture of a small amount of tetragonal martensitic structure. The signals from the martensitic phase in sample 300 is less pronounced in comparison with that in sample 250, indicating a smaller amount of martensitic phase in sample 300.

Figure 2(a) displays the temperature-dependent zero-field-cooled (ZFC) and field-cooled (FC) magnetization measured under a field of 0.02 T for the three samples O, 250 and 300. One can find that the thermo-magnetization curves drop suddenly on cooling and increase drastically on heating, which is indicative of the martensitic and reverse transformation. With subsequent annealing of the sample at 250 and 300 °C for 3 h, the martensitic transformation temperature T_M gradually moves to lower temperatures. It was determined that T_M appears at 314 K, 294 K and 283 K for samples O, 250 and 300, respectively, while the thermal hysteresis remains nearly unchanged, ~10 K. (Here, T_M is defined as the temperature corresponding to the maximal slope of the M–T curve under 0.02 T on cooling.) The location of T_M indicates that sample O shows the martensitic structure at room temperature, while the other two show the cubic austenitic structure. Due to the lower T_M of sample 300, the admixed martensitic structure at room temperature in sample 300 is less pronounced than that in sample 250. All these are consistent with the XRD results (figure 1).

From figure 2(a), one can note that the ZFC curves do not coincide with FC curves below a certain temperature (T_f).

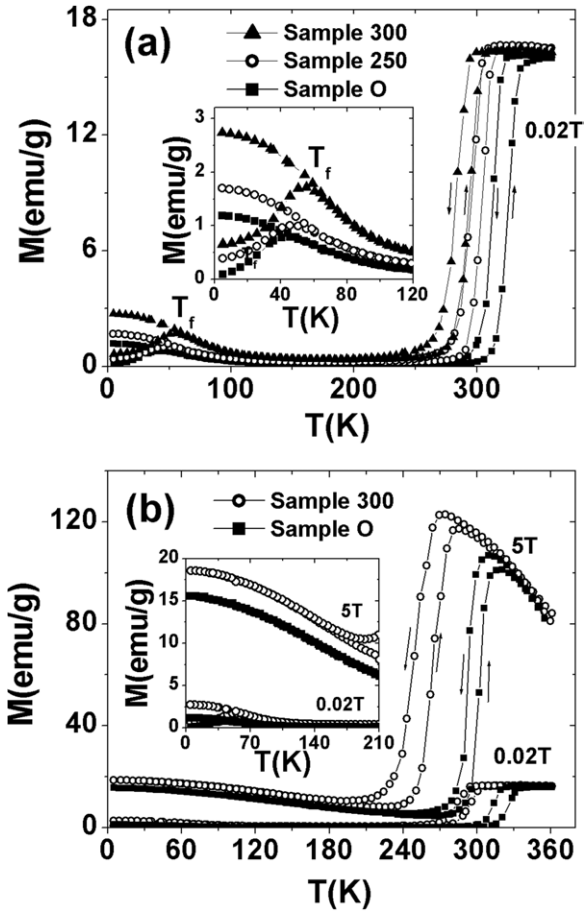

Figure 2. (*a*). The temperature dependence of zero-field-cooled (ZFC) and field-cooled (FC) magnetization (M–T curve) under a field of 0.02 T for sample O (fresh sample), sample 250 (annealed at 250 °C for 3 h) and sample 300 (annealed at 300 °C for 3 h). The inset shows the details of M–T curves at low temperatures. (*b*) Temperature-dependent magnetization measured under 5 T compared with that under 0.02 T for samples O and 300. The arrows indicate the heating/cooling path.

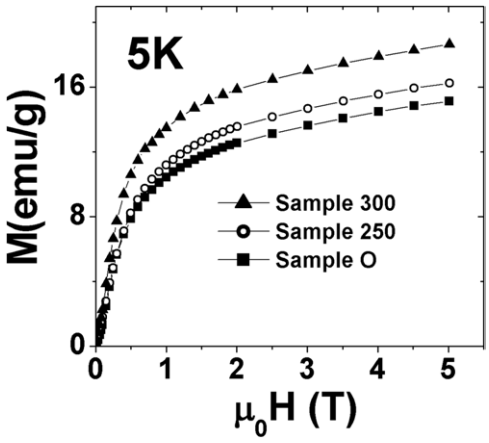

Figure 3. The magnetic field dependent magnetization (M–H curves) measured at 5 K under a field of 5 T for sample O (fresh sample), sample 250 (annealed at 250 °C for 3 h) and sample 300 (annealed at 300 °C for 3 h).

The ZFC magnetization shows a maximum at T_f while FC magnetization shows a monotonic increase below T_f, which may be indicative of a cluster-glass-like magnetic behaviour [10, 14]. Intriguingly, the cluster glass freezing temperature T_f increases with increase of the annealing temperature, appearing at 42 K, 47 K and 55 K for samples O, 250 and 300, respectively. The inset of figure 2(*a*) exhibits the details of M–T curves at low temperatures. One can find the gradual increase of T_f with increasing annealing temperature, which may indicate the growth of the ferromagnetic (FM) spin structure [15]. Figure 3 displays magnetic-field-dependent magnetization (M–H curves) measured at 5 K up to a field of 5 T. One can find the magnetization of the martensitic state is enhanced by annealing, verifying the growth of the FM structure with increasing annealing temperature. The magnetization of sample 300 under 5 T ($\sim$18.6 emu g^{-1}) is larger than that of sample O ($\sim$15.1 emu g^{-1}) by $\sim$19%. Moreover, the unsaturation of the magnetization up to 5 T field (see figure 3) also reflects the cluster-glass-like magnetic behaviour [14]. In a Mn-rich alloy, Mn–Mn antiferromagnetic (AFM) coupling occurs due to the appeared Mn–Mn nearest neighbours. The frustration of random competing Mn–Mn AFM and FM interactions may lead to cluster-glass-like behaviour. The as-prepared samples contain stress since they quenched from 1173 K to ice water at the end of preparation. Subsequently annealing even at low temperatures may modify the atom site/ordering and favour the FM coupling through relaxing the stress, resulting in an increase in T_f and an enhanced magnetization.

There are many technical and physical factors that affect the martensitic transition temperature T_M. Previous studies indicated that the martensitic transition takes place when the Fermi surface reaches the Brillouin zone boundary [16, 17]. The change in valence electron concentration alters the topology of the Fermi surface and drives the occurrence of structural instabilities. Therefore, modifying e/a is a common way to adjust T_M. However, in addition to the effect of e/a on T_M, many other factors, such as grain size, stress distribution at phase boundaries and atomic ordering [12] can also affect T_M. A recent investigation on ferromagnetic shape memory alloy FePd indicated that T_M is dependent on grain size [18]. It was found that T_M decreases as the grain size becomes smaller. However, for the present alloy $Ni_{45}Co_5Mn_{36.6}In_{13.4}$, scanning electron microscope (SEM) results indicate that the average grain size does not get smaller but remains nearly unchanged upon annealing. Hence, the decrease in T_M could not be ascribed to the grain size. The reason may be related to the stress relaxation and atomic order modification. The formed stress during the quenching process was relaxed to some extent depending on the annealing temperature and duration, which may modify atom site/ordering, Mn–Mn distance, as well as lattice symmetry. As a result, the Mn–Mn exchange coupling, Fermi surface and the Brillouin zone boundary may be changed. A proposed origin for martensitic structural transformation comes from the contact between Fermi surface and Brillouin zone boundary. This mechanism is originally invoked for CuAu [19], but has been supported by comparison in several NiMn-based Heulser systems [16], such as Ni_2MnAl, Ni_2MnGa and $Ni_2Mn_{1-x}V_x$. The subtle change of lattice caused by stress relaxation and atomic order

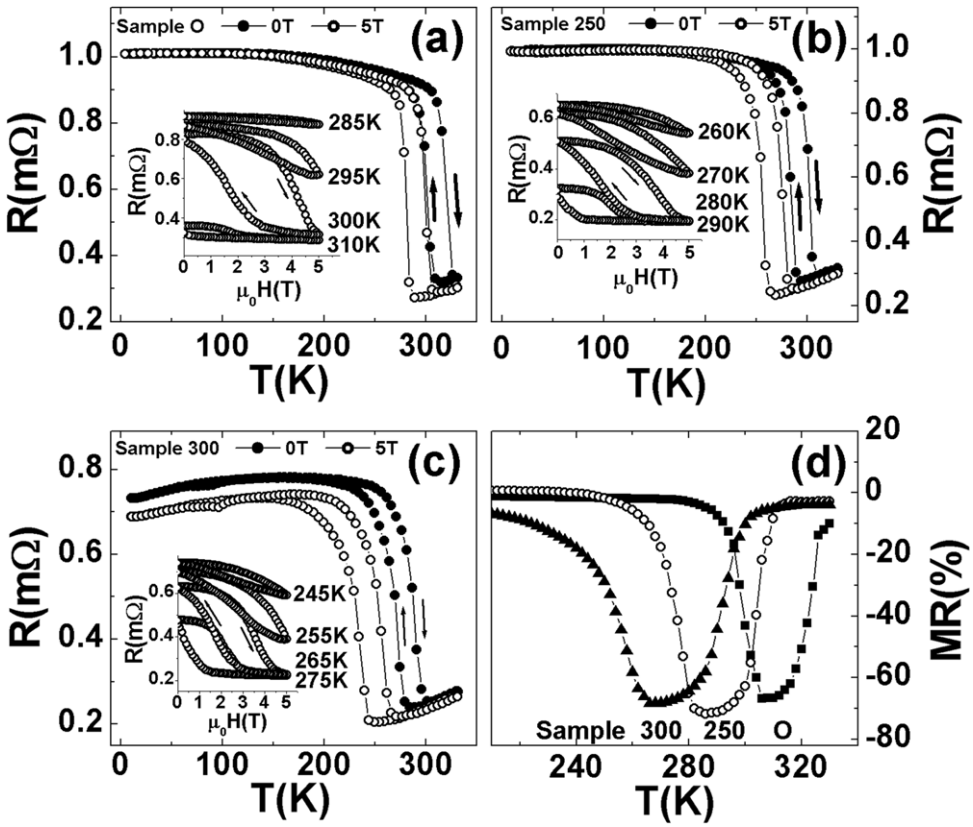

Figure 4. Temperature-dependent resistance under 0 T ($R_{0\,T}$) and 5 T ($R_{5\,T}$) for (*a*) sample O (fresh sample), (*b*) sample 250 (annealed at 250 °C for 3 h) and (*c*) sample 300 (annealed at 300 °C for 3 h). The corresponding inset shows the field-dependent resistance at different temperatures for the samples. (*d*) Temperature-dependent MR $[(R_{5\,T} - R_{0\,T})/R_{0\,T}]$ under 5 T for the three samples. The arrows indicate the heating/cooling path, as well as the field ascending/descending path.

modification may alter the Brillouin zone boundary upon annealing. All these combined elements result in a change in martensitic transformation, leading to the decrease in T_M.

Figure 2(*b*) displays the temperature-dependent magnetization under 5 T compared with that under 0.02 T for samples O and 300 (for the sake of clarity, the data of sample 250 were not plotted). Around T_M the austenitic state of both samples shows strong ferromagnetism while the martensitic state shows small magnetization under 5 T. These behaviours are very similar to the report in [5]. The magnetization change, ΔM, across martensitic transformation reaches $\sim$110 emu g^{-1}, $\sim$111 emu g^{-1} and $\sim$112 emu g^{-1} for samples O, 250 and 300, respectively. Such large ΔM results in a large Zeeman energy, $\mu_0 \Delta M \cdot H$, which pushes T_M to lower temperatures at a rate of 4.8 K T^{-1}, 5.4 K T^{-1} and 6.8 K T^{-1}, and the T_M under 5 T locates at 290 K, 267 K and 249 K for samples O, 250 and 300, respectively. One can find that the driving rate of T_M by a magnetic field does not drop but shows an obvious increase upon annealing. These results clearly demonstrate that the annealed samples still retain the strong metamagnetic properties although the magnetization of the martensitic phase around T_M slightly increases compared with the as-prepared sample. The increase in the magnetization under 5 T can be found from the details shown in the inset of figure 2(*b*).

As is well known, transport properties of intermetallic compounds are determined by electron–phonon, electron-spin, electron–electron and electron-defect scattering. The simultaneous changes in magnetism and structural transformation should be accompanied by a change in transport resistance. Figures 4(*a*), (*b*) and (*c*) display temperature-dependent resistance under 0 T ($R_{0\,T}$) and 5 T ($R_{5\,T}$) for samples O, 250, and 300, respectively. The corresponding inset shows the field-dependent resistance at different temperatures. One can note that an abrupt increase in resistance occurs around the martensitic transformation. The origin of the drastic increase in resistance can be related to the variation of the density state (DOS) in the vicinity of the Fermi level. The nature of the low magnetization in the martensitic state remains controversial. Some people believe that it is of the paramagnetic phase [20], while others think of it as being of a mixture of ferro- and antiferromagnetic phases [21, 22]. A recent neutron-polarization-analysis experiment [23] has detected antiferromagnetic correlations at temperatures lower than T_M for some Mn-rich alloys with metamagnetic properties, such as $Ni_{50}Mn_{40}Sb_{10}$ and $Ni_{50}Mn_{37}Sn_{13}$. Similarly to the materials that undergo antiferromagnetic transition [24], the formation of superzone boundary gaps may alter the density of the electronic states near the Fermi surface, leading to an enhancement of transport resistance during martensitic transformation. Furthermore, the increased interfacial scattering at the twin-boundaries may also contribute to the drastic increase in resistance upon martensitic transformation. With T_M shifting to lower temperature under an external field, a negative MR was observed. Figure 4(*d*) plots the deduced

temperature-dependent MR $[(R_{5\,\mathrm{T}} - R_{0\,\mathrm{T}})/R_{0\,\mathrm{T}}]$ under a 5 T field for the three samples. One can note that the maximal MR under 5 T reaches about 67%, 72%, 69% at 306 K, 286 K, 266 K, for samples O, 250, 300, respectively. It indicates that upon simply low-temperature annealing, the temperature, at which MR peaks, can be modulated over a wide range near room temperature while the large magnitude of MR does not drop but slightly increases. Furthermore, from each inset of figures 4(*a*), (*b*) and (*c*), one can find that the MR behaviour is fully reversible for all the three samples. The resistance can return to its original value after a field cycle up to 5 T. This reversible feature of MR is attractive in respect of real applications. Another interesting feature is that little change in electrical resistance is observed under a field of 5 T in the temperature range where the martensitic state prevails for both samples O and 250 (figures 4(*a*) and (*b*)), but an obvious drop of resistance appears (figure 4(*c*)) in sample 300. This may be related to the growth of ferromagnetic domains, and the altering of atomic ordering and twin-boundaries caused by stress relaxation, taking into account the relatively higher annealing temperature for sample 300. All these results also demonstrate the fact that the sample starts to lose stabilities as it is heated to 250 °C.

4. Conclusions

In summary, the effect of low-temperature annealing on metamagnetic properties and MR behaviours was investigated in $Ni_{45}Co_5Mn_{36.6}In_{13.4}$ alloys. We found that post-annealing at temperatures $\leqslant$300 °C can considerably affect magnetic properties and shift T_M to lower temperatures while retaining the strong metamagnetic properties. Stress relaxation, caused by annealing, may modify atom site/ordering, Mn–Mn distance, as well as lattice symmetry, hence affect martensitic transformation and magnetic properties. The strong metamagnetic behaviour is accompanied with a large MR. By simply adjusting annealing temperature, large MR can take place over a wide temperature range near room temperature. The fully reversible character of MR against magnetic field remains unchanged upon annealing. All these characteristics provide this novel alloy with more innovative applications.

Acknowledgments

This work has been supported by the National Natural Science Foundation of China, Hi-Tech Research and Development program of China, the Knowledge Innovation Project of the Chinese Academy of Sciences and the National Basic Research of China.

References

[1] Yuasa S, Nagahama T, Fukushima A, Suzuki Y and Ando K 2004 *Nature Mater.* **3** 868
[2] Chatterji T (ed) 2004 *Colossal Magnetoresistive Manganites* (Dordrecht: Kluwer)
[3] Morellon L, Stankiewicz J, Garcia-Landa B, Algarabel P A and Ibarra M R 1998 *Appl. Phys. Lett.* **73** 3462
[4] Mira J, Rivadulla F, Rivas J, Fondado A, Guidi T, Caciuffo R, Carsughi F, Radaelli P G and Goodenough J B 2003 *Phys. Rev. Lett.* **90** 097203
[5] Kainuma R *et al* 2006 *Nature* **439** 957
[6] Karaca H E, Karaman I, Basaran B, Ren Y, Chumlyakov Y I and Maier H J 2009 *Adv. Funct. Mater.* **19** 983
[7] Han Z D, Wang D H, Zhang C L, Tang S L, Gu B X and Du Y W 2006 *Appl. Phys. Lett.* **89** 182507
[8] Yu S Y, Liu Z H, Liu G D, Chen J L, Cao Z X, Wu G H, Zhang B and Zhang X X 2006 *Appl. Phys. Lett.* **89** 162503
[9] Sharma V K, Chattopadhyay M K, Shaeb K H B, Anil Chouhan and Roy S B 2006 *Appl. Phys. Lett.* **89** 222509
[10] Krenke T, Acet M, Wassermann E, Moya X, Mañosa L and Planes A 2006 *Phys. Rev.* B **73** 174413
[11] Khan M, Dubenko I, Stadler S and Ali N 2004 *J. Phys.: Condens. Matter* **16** 5259
[12] Ito W, Nagasako M, Umetsu R Y, Kainuma R, Kanomata T and Ishida K 2008 *Appl. Phys. Lett.* **93** 232503
[13] Kustov S, Corró M L, Pons J and Cesari E 2009 *Appl. Phys. Lett.* **94** 191901
[14] Itoh M, Natori I, Kubota S and Motoya M 1994 *J. Phys. Soc. Japan* **63** 1486
[15] Wohlfarth E P (ed) 1980 *Ferromagnetic Materials* (Amsterdam: North-Holland)
[16] Webster P J, Ziebeck K R A, Town S L and Peak M S 1984 *Phil. Mag.* B **49** 295
[17] Entel P, Buchelnikov V D, Khovailo V V, Zayak A T, Adeagbo W A, Gruner M E, Herper H C and Wassermann E F 2006 *J. Phys. D: Appl. Phys.* **39** 865
[18] Seki K, Kura H, Sato T and Taniyama T 2008 *J. Appl. Phys.* **103** 063910
[19] Sato H and Toth R S 1961 *Phys. Rev.* **124** 1833
[20] Schlagel D L, Yuhasz W M, Dennis K W, McCallum R W and Lograsso T A 2008 *Scr. Mater.* **59** 1083
[21] Krenke T, Duman E, Acet M, Wassermann E F, Moya X, Mañosa L, Planes A, Suard E and Bachir Ouladdiaf 2007 *Phys. Rev.* B **75** 104414
[22] Sharma V K, Chattopadhyay M K, Kumar R, Ganguli T, Tiwari P and Roy S B 2007 *J. Phys.: Condens. Matter* **19** 496207
[23] Aksoy S, Acet M, Deen P P, Mañosa L and Planes A 2009 *Phys. Rev.* B **79** 212401
[24] Zhang Y Q, Zhang Z D and Aarts J 2004 *Phys. Rev.* B **70** 132407